Research Square

Preprints are preliminary reports that have not undergone peer review.
They should not be considered conclusive, used to inform clinical practice,
or referenced by the media as validated information.

Molecular Dynamics Insight into Temperature-Modulated Microstructure and Mechanical Behavior of Cu–SiO_2 Hybrid Bonding Interfaces

Jinzhong Zhang
Qinghai Water Resources and Hydropower Survey, Planning, Design and Research Institute Co., Ltd
Yujie Xue
Xidian University
Shiren La
Qinghai Minzu University
Yang Shi
shiyang@xidian.edu.cn

Xidian University

Research Article

Keywords: 3D packaging, Hybrid bonding, Molecular dynamics simulation, Thermo-compression bonding, Mechanical properties

Posted Date: November 25th, 2026

DOI: https://doi.org/10.21203/rs.3.rs-11436373/v1

License: This work is licensed under a Creative Commons Attribution 4.0 International License.
Read Full License

Additional Declarations: No competing interests reported.

Molecular Dynamics Insight into Temperature-Modulated Microstructure and Mechanical Behavior of Cu–SiO_2 Hybrid Bonding Interfaces

Jinzhong Zhang[a], Yujie Xue[b], Shiren La[c], Yang Shi[b,*]

[a]Qinghai Water Resources and Hydropower Survey, Planning, Design and Research Institute Co., Ltd, Xining, 810001, China

[b]School of Mechano-Electronic Engineering, Xidian University, Xi'an, 710071, China

[c]School of Civil and Transportation Engineering, Qinghai Minzu University, Xining, Qinghai, 810007, China

ABSTRACT

This work presents a systematic atomistic investigation of temperature-induced microstructural evolution and mechanical property modulation in Cu–SiO_2 hybrid bonding heterogeneous interfaces. A computational atomic model, consisting of copper pillars embedded within an amorphous SiO_2 substrate, is established to replicate the thermo-compression bonding process, enabling quantitative evaluation of interfacial atomic diffusion kinetics and crystalline phase structural evolution. The simulation results reveal a strong temperature dependence of structural ordering and mechanical performance at the Cu-Cu bonding interface. Elevating the bonding temperature from 250 °C to 350 °C effectively promotes interfacial atomic diffusion, which increases the fraction of face-centered cubic phase from 44.8% to 49.0% and suppresses disordered atomic configurations, delivering an optimal elastic limit of the Cu-Cu interface at 350 °C. Further increasing the temperature to 400 °C introduces intense thermal perturbation, which disrupts atomic ordering and degrades the structural uniformity of the metallic interface. In comparison, the covalent network structure of the SiO_2-SiO_2 interface endows the dielectric interface with excellent structural and mechanical stability throughout the investigated temperature range. The findings may reliable atomistic insights and a theoretical basis for the parametric optimization of thermo-compression bonding and the quality enhancement of heterogeneous interfacial bonding.

Key words: 3D packaging; Hybrid bonding; Molecular dynamics simulation; Thermo-compression bonding; Mechanical properties.

*Author to whom correspondence should be addressed: shiyang@xidian.edu.cn

I. Introduction

As integrated circuit feature sizes approach physical limits, three-dimensional (3D) integration technology has become a key pathway for extending Moore's Law and enhancing system performance and integration density [1]. Among these technologies, hybrid bonding enables the heterogeneous integration of copper interconnects and dielectric layers in a single process step, providing a core solution for high-density vertical interconnections [2-4]. This technique simultaneously forms electrical connections between copper conductors and mechanical bonds between silicon dioxide dielectric layers, thereby constructing three-dimensional interconnect structures with integrated electrical, thermal, and mechanical functionalities. However, the bonding strength at the Cu–SiO_2 heterogeneous interface directly determines the electrical performance and long-term reliability of the interconnects [5]. This strength is highly dependent on the complex coupling of multiple parameters such as temperature and pressure during thermo-compression bonding, yet the underlying microscopic mechanisms remain unclear. Therefore, how to precisely control bonding parameters to predict and optimize the mechanical properties of heterogeneous interfaces is a key scientific issue that must be addressed to advance this technology toward mature application.

To address this issue, researchers have conducted in-depth investigations from both experimental and simulation perspectives. Experimentally, studies have focused on surface treatment, bonding temperature, and material system optimization. For example, Kim *et al* [6] found that O_2 plasma treatment effectively enhances bonding strength, but excessive power increases surface roughness due to ion bombardment. He *et al* [7, 8] developed a low-temperature activation scheme to achieve high-quality bonding below 200°C. Ou *et al* [9] demonstrated that moderately increasing bonding temperature (200–300°C) promotes copper grain coarsening and interface healing. Ong *et al* [10] utilized (111)-oriented copper surfaces to achieve low-resistance, highly stable connections under low-temperature and low-pressure conditions. Kuo *et al* [11] introduced nanotwinned copper to further reduce

the thermal budget of the process. Although experimental characterizations can reveal the intrinsic influences of bonding processes, they suffer from limited testing techniques and high experimental costs. By contrast, numerical simulation enables efficient pre-verification of product design schemes, facilitating structural optimization and mass production implementation.

To address experimental limitations, simulation methods have become essential tools for understanding interface behavior. Specifically, finite element analysis guides process optimization at the macroscale. For instance, Ren *et al* [12] established a model considering non-uniform inputs to determine annealing windows for void-free interfaces. Ji *et al* [13] quantified interfacial peeling stress induced by copper protrusion using a three-dimensional finite element model. Ni *et al* [14] optimized stress distribution through structural design. Sekhar *et al* [15] considered various design, material, and process parameters in C2W-HB processes to enhance the integrity of bonded dielectric layers and Cu pads. Cheemalamarri *et al* [16] used ANSYS to study the dependence of copper expansion on various surrounding dielectric conditions, metal pad spacing, and shapes. The finite element method has achieved considerable advances in macroscopic mechanical analysis, yet it struggles to characterize microscale interfacial characteristics at the atomic level. Molecular dynamics (MD) simulations have thus become an effective means to explore these microscopic mechanisms [17-21]. For metal bonding, Xydou *et al* [22] elucidated the synergistic effects of temperature and pressure on interfacial atomic diffusion and void closure. Wu *et al* [23, 24] revealed the influence of surface morphology and microstructure. Tatsumi *et al* [25] emphasized the role of crystal orientation on interfacial densification. For dielectric materials, Hiller *et al* [26] investigated a two-dimensional SiO_2/AlO_x interface effect. Additionally, studies evaluating interfacial mechanical properties through simulated tensile tests have been widely conducted [27, 28] For example, Liu *et al* [29] analyzed the tensile behavior and strength variation at Cu/Al interfaces, Ren *et al* [30] revealed deformation mechanisms at Al–Cu interfaces from an atomic perspective, and Hu

et al [31] highlighted the decisive influence of interfacial structure on the properties of nanoscale components.

Despite significant progress, a fundamental limitation persists: most atomic-scale simulations focus on homogeneous interfaces such as Cu–Cu or SiO_2–SiO_2 bonding. Studies that simulate the simultaneous bonding of Cu and SiO_2—two materials with vastly different properties—under the same thermo-compression process and the synergistic evolution of their heterogeneous interfaces remain scarce. This results in a lack of systematic understanding of the competitive formation mechanisms at metal–dielectric interfaces and their impact on the overall mechanical properties of composite interfaces in real hybrid bonding. To address this gap, this study constructs a MD model for the simultaneous bonding of Cu and SiO_2 heterogeneous materials under identical thermos-compression conditions, accurately replicating the core physical processes of hybrid bonding. By systematically varying key parameters such as temperature, we simulate the synergistic formation of Cu–Cu metallic interfaces and SiO_2–SiO_2 covalent interfaces. Subsequently, directed tensile tests are performed on the bonded composite interface to quantitatively obtain the stress–strain response and adhesion strength of the heterogeneous interface. This research reveals, at the atomic scale, the intrinsic mechanisms through which process parameters determine the final mechanical properties of hybrid bonding interfaces by regulating interfacial atomic diffusion and bonding behavior. The findings may provide a new theoretical foundation for optimizing bonding processes and reliability design in three-dimensional integration.

2. MD simulation of Cu-SiO_2 hybrid bonding process

2.1. Simulation framework and process parameter configuration

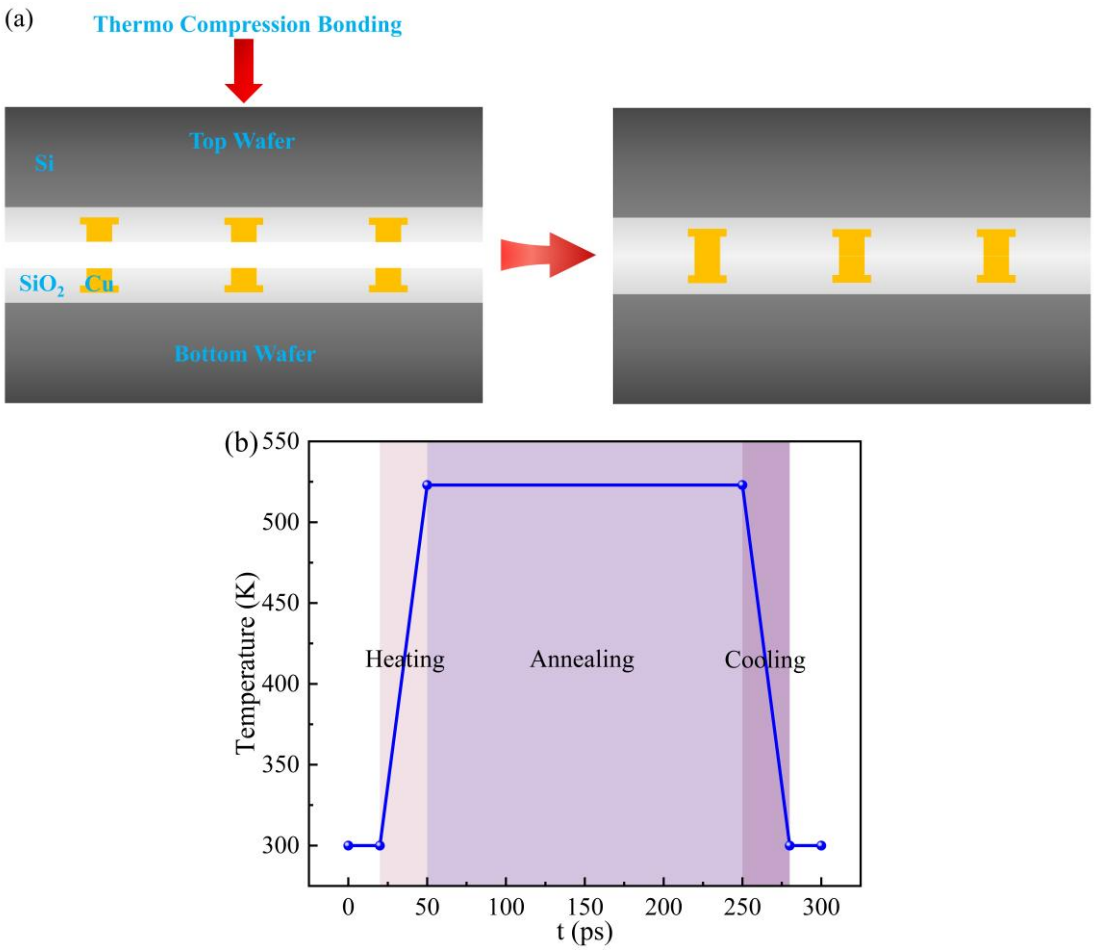

Figure 1. (a) Schematic of the hybrid bonding structure in 3D packaging; (b) Temperature control profile.

The molecular dynamics simulation in this study aims to reveal, at the atomic scale, the core mechanisms of Cu/SiO_2 hybrid bonding in 3D integration. As shown in Fig. 1(a), hybrid bonding is an advanced heterogeneous integration technique that combines the formation of covalent bonds (Si–O–Si) at SiO_2 interfaces with thermally driven diffusion and bonding of Cu–Cu metal contacts. The macroscopic performance of the bonded structure depends critically on the temperature parameters applied during thermo-compression bonding. The technique typically employs plasma activation to promote surface bonding, followed by thermally driven diffusion and recrystallization of copper atoms, ultimately yielding a high-strength,

low-resistance interconnect structure. The simulation is based on a representative thermo-compression bonding process, the core of which is the coordinated control of temperature and pressure. As illustrated in Fig. 1(b), the process is abstracted and divided into three consecutive stages [32]:

(1) Heating and contact stage (0–50 ps):

The system temperature is rapidly increased from an initial 300 K to the target bonding temperature. This stage aims to activate interfacial atoms, overcome surface energy barriers, and promote initial physical contact between the Cu and SiO_2 surfaces.

(2) High-temperature/high-pressure annealing stage (50–250 ps):

The system is maintained at a constant, preset high temperature and high pressure. This stage constitutes the core of interfacial bonding and drives two key processes: (i) dehydration condensation between hydroxyl groups on the SiO_2 surfaces, forming strong covalent Si–O–Si bonds; and (ii) thermally and stress-driven diffusion, rearrangement, and recrystallization of copper atoms across the interface, establishing metallic connections.

(3) Cooling and relaxation stage (250–300 ps):

Temperature and pressure are controllably and gradually reduced to ambient conditions. This stage allows the system energy to minimize, alleviates residual stresses caused by thermal mismatch, stabilizes the post-bonding interface structure, and ensures its thermodynamic stability.

Within this process framework, temperature is the key independent variable controlling interfacial bond formation. To systematically investigate their influence, simulations were conducted over practical process windows: bonding temperatures from 250 °C to 400 °C. By simulating the complete dynamic process—from initial contact through bonding to stabilization—across different parameter combinations,

this study lays the groundwork for subsequent analysis of how temperature affect atomic structure, bonding state, and the final mechanical properties of the interface.

2.2 Construction of the MD model

This study employed the Large-scale Atomic/Molecular Massively Parallel Simulator (LAMMPS) platform in conjunction with the Open Visualization Tool (OVITO) to construct an atomic-scale molecular dynamics model of the hybrid bonding process. The aim was to investigate the evolution and distribution of interfacial crystalline and phase structures during bonding. The specific modeling and simulation workflow are detailed below:

(1) Initial model construction

First, a 3D periodic model of an amorphous SiO_2 substrate was constructed using the Build Symmetry tool in Materials Studio 2020 [33]. The substrate dimensions were set to 98 Å × 98 Å × 42 Å (x × y × z), a size determined through testing to effectively minimize finite-size boundary effects during simulation. A schematic of the model structure is presented in Fig. 2(a). To accurately describe the covalent interactions of Si–O bonds, the Tersoff potential function was employed [34, 35]. Its total potential energy E is expressed as:

$$E = \frac{1}{2}\sum_{i}\sum_{j\neq i} f_C(r_{ij}+\delta)\left[f_R(r_{ij}+\delta) + b_{ij} f_A(r_{ij}+\delta)\right], \quad (1)$$

where δ represents the atomic type offset, used to adjust the interactions between different atomic species; $f_C(r)$ denotes the cutoff function in the interaction potential between Si and O, ensuring a smooth attenuation of short-range interactions; $f_R(r)$ represents the short-range repulsion between atomic nuclei; $f_A(r)$ describes the long-range attractive behavior; and b_{ij} is the bond-order correction coefficient.

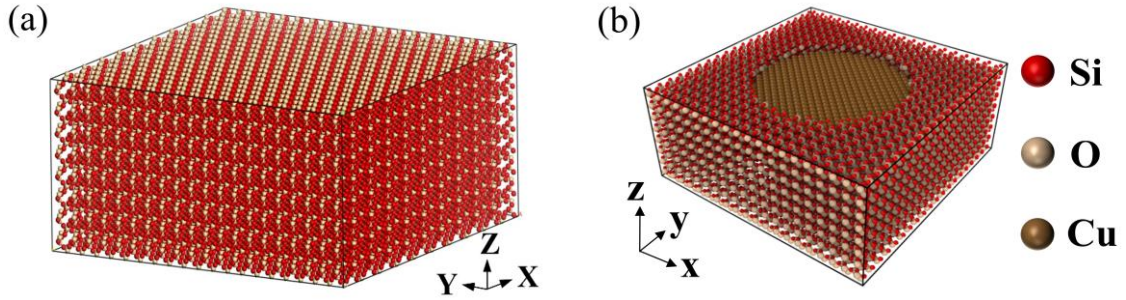

Figure 2. (a) 3D periodic structure of the SiO_2 substrate model;(b) Schematic of the initial configuration of the "lower wafer" Cu–SiO_2 heterogeneous structure.

(2) Construction of the copper pillar structure

To create the copper interconnect structure within the SiO_2 substrate, the delete_atoms command in LAMMPS was used to remove a cylindrical region (centered at (49 Å, 49 Å) with a radius of 30 Å, extending axially from 10 Å above the bottom surface of the substrate through the entire thickness to the top surface). Subsequently, this cavity was filled with copper atoms, covering a height range from 10 Å to 41 Å, leaving a 1 Å gap from the top surface of the substrate (as shown in Fig. 2(b)). This design is based on the fact that copper has a higher coefficient of thermal expansion than SiO_2, which under radial confinement during thermo-compression bonding will induce axial expansion, thereby promoting complete bonding. The interactions between copper atoms were described using the Embedded Atom Method (EAM) potential [36], where the total energy E_i for atom i is expressed as [37]:

$$E_i = F_\alpha\left(\sum_{j\neq i}\rho_\beta(r_{ij})\right) + \frac{1}{2}\sum_{j\neq i}\emptyset_{\alpha\beta}(r_{ij}), \tag{2}$$

where $F_\alpha(.)$ is the embedding energy function, representing the energy required to embed copper atom i into the local electron density contributed by its neighboring atoms; $\emptyset_{\alpha\beta}$ is the pairwise potential term, describing the pair-wise interaction energy between atom i and all surrounding atoms j; and $\rho_\beta(r_{ij})$ is the contribution of atom j to the local electron density at atom i at a distance r_{ij} (approximately 2.55 Å in this study).

(3) Interfacial interaction potential functions

For the short-range interactions at the bonding interface between Cu–Si and Cu–O, a reactive charge-optimized many-body potential was employed [38-42]. This potential function expresses the total energy of the system as a functional of dynamic charge distribution and many-body geometric configurations:

$$E_T = \sum_i [E_i^{self}(q_i) + \sum_{j>i} [E_{ij}^{short}(r_{ij}, q_i, q_j) + E_{ij}^{Coul}(r_{ij}, q_i, q_j)] + E^{polar}(q_i, r_{ij}) + E^{vdW}(r_{ij}) + E^{barr}(q_i) + E^{corr}(r_{ij}, \theta_{jik})], \quad (3)$$

where E_T is the total energy of the atomic system; E_i^{self} is the self-energy of atom i, including its ionization energy and electron affinity; E_{ij}^{short} is the bond-order potential between atoms i and j; E_{ij}^{Coul} represents Coulombic interactions; E^{polar} is the polarization term for the organic system; E^{vdW} denotes the van der Waals energy; E^{barr} is the charge barrier function; and E^{corr} is an angular correction term.

(4) Assembly of the bonding system and simulation setup

The constructed "lower wafer" model was rotated 180° around the x-axis to create a symmetric "upper wafer" model. Both models were then merged using the read_data command in LAMMPS to form the complete initial bonding system, as shown in Fig. 3(a). To examine the atomic distribution at the bonding interface, a cross-section was taken at the plane x = 49 Å, and the atomic arrangement in the yz plane was visualized using OVITO, as presented in Fig. 3(b).

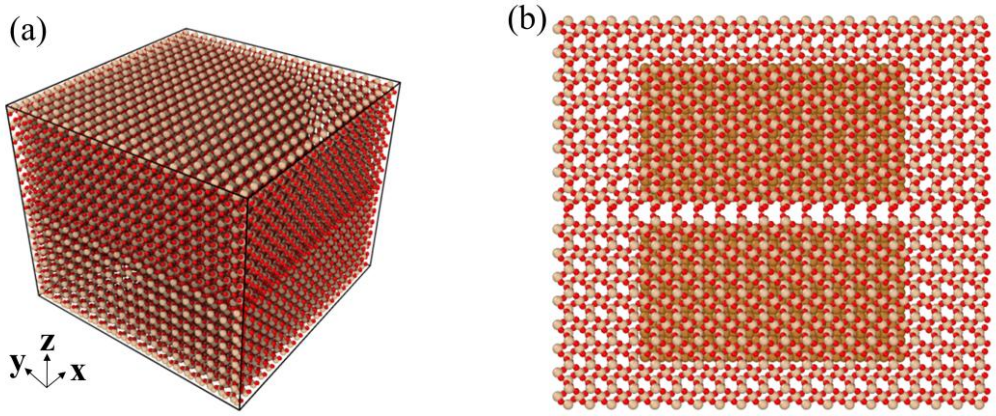

Figure 3. Overview of the molecular dynamics simulation for hybrid bonding. (a) Schematic of the initial three-dimensional structure of the complete bonding system; (b) Atomic arrangement in the yz cross-section at x = 49 Å (used for observing the interfacial structure).

(5) Boundary conditions and ensemble control

Periodic boundary conditions (p boundary) were applied in all three directions (X, Y, Z) to simulate an infinitely extended structure and maintain constant density. The Nosé–Hoover thermostat was used to regulate the temperature of the entire system. After energy minimization, the system was first relaxed to the initial equilibrium temperature under the NVT ensemble. Subsequently, during the bonding simulation stage, the target temperature was maintained using the fix_npt command while controlling temperature fluctuations. To simulate the thermo-compression bonding process, anisotropic pressure was applied within the NPT ensemble. In the X and Y directions (in-plane directions), constant pressure (or zero pressure) was maintained, while a constant positive pressure was applied in the Z direction (perpendicular to the bonding interface) to drive the close contact and reaction of the interfacial atoms between the upper and lower wafers.

3. Results and discussion

3.1 Relaxation and convergence verification of the simulation system

After completing the model construction, the conjugate gradient algorithm in LAMMPS was employed to perform energy minimization on the system, aiming to eliminate unreasonable atomic overlaps and local stresses. The convergence tolerances for both energy and force were set to 1.0×10^{-10}, with a maximum iteration step count of 10,000. This method iteratively optimizes atomic positions, gradually driving the system potential energy toward a local minimum. The convergence process of the total system energy over simulation time is illustrated in Fig. 4. The initial energy was approximately -2.71×10^{5} eV, which rapidly decreased within about 4 ps and gradually stabilized, eventually converging near -3.19×10^{5} eV—a reduction of approximately 17.6%. This indicates that the system has reached a stable low-energy state.

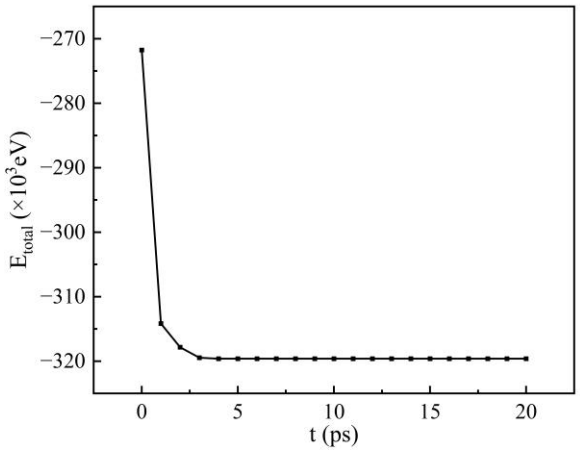

Figure 4. Convergence curve of the total energy of the hybrid bonding system.

To further analyze the relaxation behavior of the interface structure, Fig. 5(a) and (b) respectively present a comparison of the atomic configurations at the Cu–Cu interface and the SiO_2–SiO_2 interface before and after relaxation. At the initial bonding moment (0 ps), the atomic arrangement at the interface was still irregular, exhibiting clear non-equilibrium characteristics. After a sufficient relaxation period of 20 ps, atomic rearrangement occurred at the interface. The Cu–Cu interface displayed a more compact metallic bonding characteristic, while the SiO_2–SiO_2 interface tended to form a stable covalent network structure.

The above results indicate that, through the energy minimization and relaxation processes, the system has achieved a stable, low-energy initial configuration. This provides a reliable structural foundation for subsequent mechanical and thermal simulations of the hybrid bonding process.

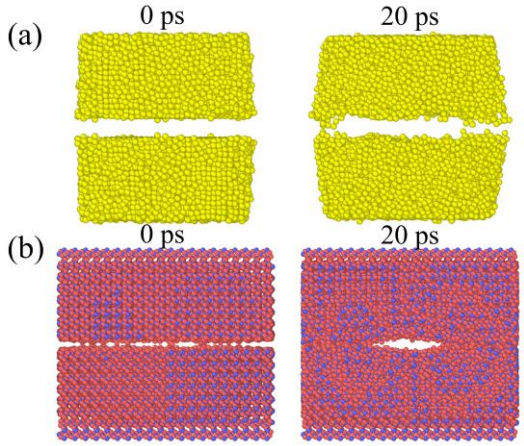

Figure 5. Evolution of atomic structures at the Cu/SiO_2 hybrid bonding interface during relaxation: (a) Cu–Cu interface; (b) SiO_2–SiO_2 interface.

This study conducted atomic-scale simulations of the annealing process at the Cu/SiO_2 heterogeneous interface under bonding conditions of 300 °C and 2 MPa. The structural evolution is illustrated in Fig. 6. Driven synergistically by temperature and pressure, significant atomic diffusion, rearrangement, and chemical bonding occurred in the interfacial region. Fig. 6(a) depicts the dynamic evolution of the Cu–Cu interface. In the initial state, a distinct physical gap was present at the interface. As annealing progressed, under sustained vertical pressure, copper atoms migrated toward the interfacial region, filling the gaps and ultimately forming a continuous, dense metallic bonding zone, indicating that metallurgical bonding had been achieved at the interface. Fig. 6(b) illustrates the structural evolution at the SiO_2–SiO_2 interface. Initial local micro-voids were observed at the interface. Under the combined thermal and mechanical effects, structural relaxation and covalent bond reconstruction occurred in the amorphous SiO_2 network, leading to gradual closure of the interface and the formation of a stable covalently bonded interface by 20 ps.

These atomic-scale observations clearly demonstrate that during the hybrid bonding process, the Cu–Cu interface and the SiO_2–SiO_2 interface exhibit distinct closure mechanisms, yet both achieve microscale cooperative closure under thermo-mechanical conditions. These results provide direct structural evidence for understanding the dynamic processes of Cu/SiO_2 hybrid bonding and establish a theoretical foundation for further systematic investigation into the optimization of key process parameters such as bonding temperature and pressure.

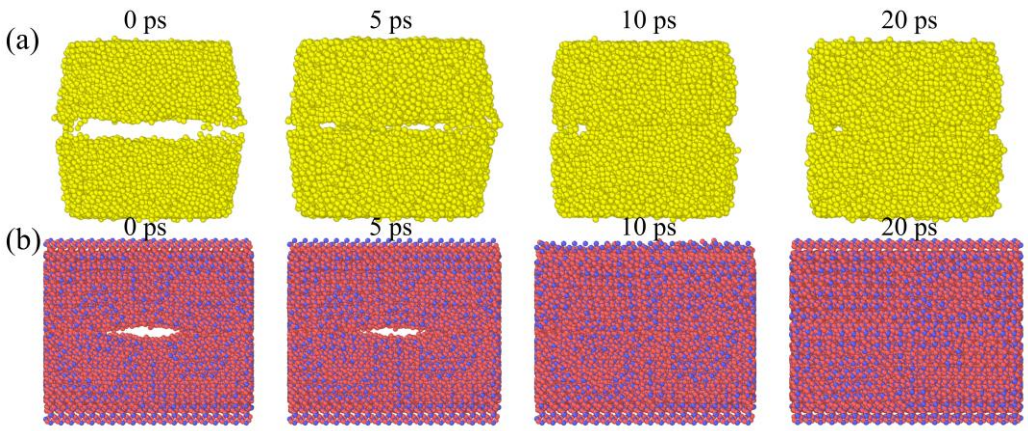

Figure 6. Evolution of the atomic structure at the Cu/SiO_2 hybrid interface during annealing: (a) Cu–Cu interface; (b) SiO_2–SiO_2 interface.

3.2 Influence of bonding temperature on hybrid bonding outcomes

To systematically investigate the effect of bonding temperature, this study conducted comparative simulations at four temperature points—250°C, 300°C, 350°C, and 400°C—under a constant bonding pressure of 2 MPa. To quantitatively characterize the diffusion kinetics of copper atoms at the interface during the annealing stage, the mean squared displacement (MSD) was adopted as the key evaluation metric. MSD is defined as the ensemble average of the squared atomic displacement and is expressed as:

$$\mathrm{MSD} = < \frac{1}{N} \sum_{i=1}^{N} [r_i(t_0 + t) - r_i(t_0)]^2 >, \tag{4}$$

where N is the number of atoms in the selected group, $r_i(t)$ denotes the position of atom i at time t, and the angle brackets $\langle \cdot \rangle$ represent the ensemble average over all atoms in the group.

For the calculation, a specific region centered on the bonding interface was defined: extending 8 Å inward from the bottom surface of the upper wafer and the top surface of the lower wafer, forming a total interfacial thickness of 16 Å. The trajectories of all copper atoms within this region were tracked, and their MSD as a function of time was computed. The evolution curves of MSD for copper atoms in this interfacial region under different temperature conditions are shown in Fig. 7. Each set of variables was simulated independently three times, and all results presented are averages of these three runs. The

calculated coefficient of variation remained below 1%, ensuring the stability and reliability of the numerical simulation results.

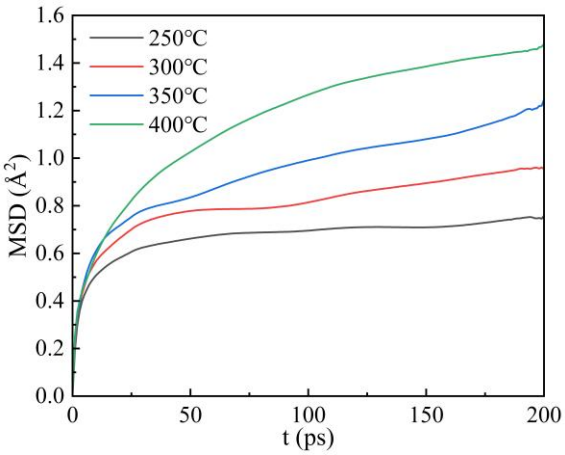

Figure 7. Evolution of the MSD at the copper-copper bonding interface under different bonding temperatures.

Analysis of the MSD based on large-scale atomic simulations reveals a significant positive correlation between the diffusion capability of interfacial copper atoms and temperature within the range of 250°C to 400°C. As temperature increases, the slope of the MSD curve becomes steeper, indicating enhanced diffusion rate and atomic mobility of copper atoms. Specifically, under conditions of 250°C and 300°C, the MSD curves tend to level off in the later stages of annealing, suggesting that atomic diffusion rapidly reaches local saturation after initial relaxation and cannot achieve long-range migration across the interface. In contrast, at 350°C and 400°C, the MSD curves maintain a consistently upward trend, indicating continuous diffusion and sufficient kinetic energy for atoms to undergo long-range migration, thereby promoting complete interfacial fusion. These results demonstrate that only when the temperature exceeds a certain threshold (e.g., ≥350°C) does the thermal activation energy become sufficient to drive sustained, large-scale atomic diffusion, enabling thorough lattice reconstruction and metallurgical bonding at the interface. Therefore, temperature serves as a critical process variable for regulating interfacial diffusion behavior, facilitating crystalline phase reconstruction, and achieving high-quality bonding.

To further elucidate the structural evolution of the bonding interface, this study

employed the Common Neighbor Analysis (CNA) method in OVITO to visualize the distribution and evolution of crystalline phase structures in the interfacial region under different temperatures. The results are shown in Fig. 8. For quantitative analysis of structural evolution, the proportions of major crystalline phases at each temperature were statistically analyzed, with detailed data presented in Table 1. To clearly illustrate the distribution and evolution of ordered lattice regions, atoms in disordered phases are omitted from the rendered views in Fig. 8. Face-centered cubic (FCC) structures are represented in green, hexagonal close-packed (HCP) structures in red, and body-centered cubic (BCC) structures in blue.

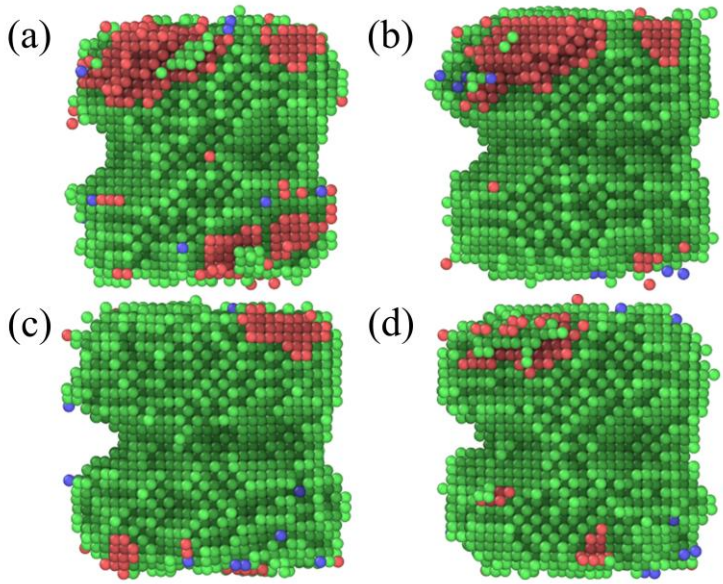

Figure 8. Visualization results of CNA at the copper-copper bonding interface under different temperatures: (a) 250°C, (b) 300°C, (c) 350°C, (d) 400°C.

Table 1. Quantitative statistical analysis of crystalline phase compositions for bonding results at different temperatures.

	Other	FCC	HCP	BCC
250°C	53.1%	44.8%	2.0%	0.1%
300°C	51.0%	47.2%	1.7%	0.1%
350°C	50.0%	49.0%	0.9%	0.1%
400°C	52.5%	46.4%	1.0%	0.1%

In the copper bonding system, each phase category carries distinct physical

significance: The disordered phase primarily comprises amorphous atoms at the interface, severely distorted lattice regions, and highly disordered structures that cannot be classified as conventional crystals. Its proportion directly reflects the incompleteness of interfacial diffusion and structural rearrangement; The FCC structure represents intact or nearly intact copper lattices, which are thermodynamically the most stable crystalline phase; The HCP structure typically appears in regions such as stacking faults, twin boundaries, or areas of localized stress concentration, serving as an indicator of crystal defects or metastable phases; The BCC structure is highly unstable in copper systems; its minimal presence may correspond to intense atomic disturbances or highly localized coordination distortions.

Combining the observations from Figs. 8(a)–(d) and the statistical results in Table 1, it is evident that as the bonding temperature increases from 250°C to 350°C, the proportion of the FCC phase gradually rises from 44.8% to 49.0%, while the disordered phase decreases from 53.1% to 50.0%, and the HCP phase declines from 2.0% to 0.9%. This trend indicates that moderate heating promotes atomic diffusion and lattice reconstruction, transforming some disordered regions into stable FCC crystalline order and improving interfacial crystallinity. However, when the temperature further increases to 400°C, the proportion of the FCC phase drops back to 46.4%, the disordered phase rebounds to 52.5%, and the HCP phase remains at approximately 1.0%. This reversal suggests that excessively high temperatures may introduce excessive thermal disturbances, which can hinder the ordering process of copper atoms and even

In summary, temperature significantly influences the crystalline phase distribution of interfacial copper atoms by regulating atomic migration and rearrangement kinetics. Within the range of 250–350°C, increasing temperature promotes the growth of the FCC phase and reduces defects. However, when the temperature becomes excessively high, enhanced thermal disorder effects hinder complete interfacial crystallization. This non-monotonic trend indicates the existence of an optimal intermediate temperature window in hybrid bonding processes, which maximizes the degree of interfacial ordering.

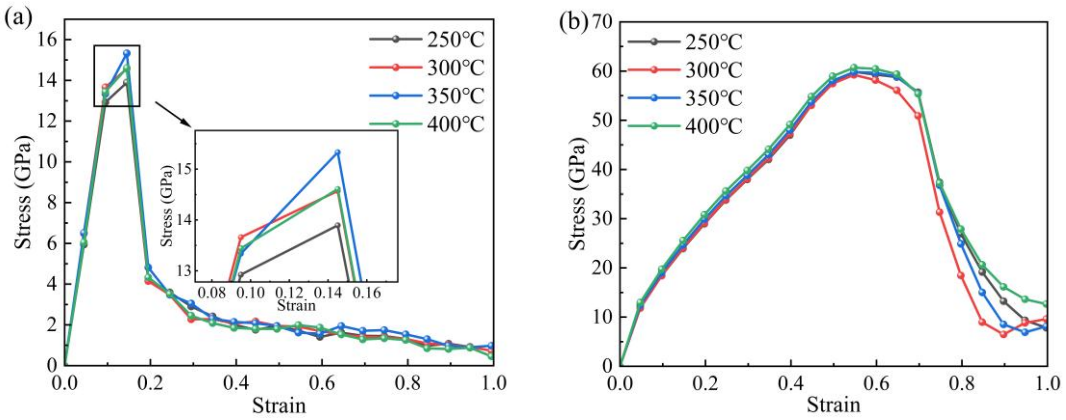

Figure 9. Stress-strain curves of the bonding interface under different temperatures: (a) Cu–Cu interface; (b) SiO_2–SiO_2 interface.

To evaluate the bonding strength at the interface, uniaxial tensile simulations were performed along the z-axis of the system at a constant strain rate of 0.05 Å/ps. The mechanical properties of both the Cu–Cu and SiO_2–SiO_2 interfaces under different temperature conditions were systematically characterized, and the corresponding stress-strain curves are shown in Fig. 9.

MD simulation results reveal distinct microscopic mechanisms governing the mechanical behavior of the two interfaces at elevated temperatures. As shown in Fig. 9(a), the elastic limit of the Cu–Cu interface exhibits a non-monotonic trend over the temperature range of 250–400 °C, first increasing and then decreasing, with a peak value of 15.33 GPa reached at 350 °C. Combined with the quantitative analysis of crystalline phase compositions presented in Table I, this temperature corresponds to the highest proportion of FCC phase in copper. In the lower temperature range (250–300 °C), atomic diffusion is insufficient, leaving more defects at the interface and resulting in a lower FCC phase fraction, which limits bonding strength. When the temperature rises to 400 °C, although atomic diffusion is enhanced, grain coarsening and dislocation activity intensify, leading to a decrease in FCC phase proportion. Therefore, 350 °C represents the optimal state with the highest FCC ordering and the best interfacial structural integrity, enabling the interface to more effectively accommodate strain during tension and exhibit the highest elastic limit.

In contrast, Fig. 9(b) shows that the stress-strain curves of the SiO_2–SiO_2 interface largely overlap across the same temperature range, indicating minimal temperature dependence in its mechanical response. This behavior stems primarily from the strongly covalent-bonded nature of silica, characterized by high bond energy and strong directionality. Within the 250–400 °C range, significant atomic rearrangement or phase transformation is unlikely, so the interfacial bonding state and deformation mechanism are hardly affected by temperature. Nevertheless, the curves display some temperature sensitivity beyond the strength limit. Specifically, the peak stress at 300 °C (59.25 GPa) is slightly lower than that at other temperatures, and its stress drop during subsequent strain softening is steeper. This suggests that at this temperature, a fraction of Si–O bonds at the interface are more prone to rupture under high strain, increasing the likelihood of interfacial structural failure.

In summary, the strength of the Cu–Cu interface varies significantly with temperature, peaking at 350 °C where the proportion of FCC phase is highest. In contrast, the SiO_2–SiO_2 interface, owing to the inherent thermal stability of covalent bonds, maintains nearly consistent mechanical properties over the 250–400 °C range. This difference indicates that for bonding processes in metal-ceramic heterogeneous systems, optimizing the temperature for the metal interface can enhance bonding strength, while for ceramic interfaces, greater attention should be paid to surface treatment and chemical compatibility control.

4. Conclusions

Through systematic molecular dynamics simulations, this study provides an atomic-scale investigation into the effects of temperature and pressure on the microstructural evolution and mechanical properties of Cu–SiO_2 hybrid bonding interfaces. The key findings are summarized as follows:

(1) Temperature exhibits a significant and non-monotonic influence on the Cu–Cu interface. Within the range of 250–350 °C, increasing temperature promotes interfacial copper atom diffusion and rearrangement, transforming disordered phases into ordered

FCC structures and enhancing interfacial strength. The optimum bonding performance was observed at 350 °C, corresponding to the highest FCC phase proportion (49.0%). However, when the temperature was raised to 400 °C, enhanced thermal disturbance reduced both the FCC phase fraction and the interfacial strength, indicating the existence of an optimal bonding temperature window.

(2) The properties of the SiO_2–SiO_2 interface are largely insensitive to thermal-mechanical parameters. Within the investigated temperature (250–400 °C) range, the SiO_2 interface maintains a stable amorphous covalent network structure, and its bonding strength remains nearly constant. This suggests that the bonding quality of SiO_2 interfaces is predominantly governed by surface chemical states rather than thermocompression conditions.

(3) A differentiated process strategy is required for heterogeneous bonding. The key to optimizing hybrid bonding performance lies in tailoring the conditions for the metal interface. It is recommended to synergistically optimize temperature (~350 °C) for the Cu–Cu interface, while for the SiO_2–SiO_2 interface, efforts should focus on surface activation and chemical treatment.

This work reveals the microscopic mechanisms through which process parameters influence heterogeneous interfaces during thermo-compression bonding and provides a theoretical foundation for precise control of practical bonding processes.

5. Declarations

5.1 Availability of data and materials

The datasets generated and analysed during this molecular dynamics study are available from the corresponding author on reasonable request.

5.2 Competing interests

The authors have no relevant financial or non-financial interests to disclose.

Acknowledgments

This research work was supported by the Qinghai Provincial Central Government

Guides Local Science and Technology Development Fund Project (2026-SF-Z48).

References

[1] Kim K S, Seo S, Kwon J Y and et al 2024 *Nature* 636 615-621

[2] Takakuwa M, Fukuda K, Yokota T and et al 2021 *Sci. Adv.* 7 eabl6228

[3] Chew S A, Vos J D and Beyne E 2024 *Nat. Rev. Electr. Eng.* 1 71-72

[4] Ke S Y, Li D K and Chen S Y 2020 *J. Phys. D: Appl. Phys.* 53 323001

[5] Lee C Y, Won C H, Jung S and et al 2025 *Electron. Mater. Lett.* 21 395-419

[6] Kim Y S, Nguyen T H and Choa S H 2022 *Micromachines* 13 537

[7] He R, Fujino M, Akaike M, Sakai T, Sakuyama S and Suga T 2017 *Appl. Surf. Sci.* 414 163-170

[8] He R, Fujino M, Yamauchi A and Suga T 2015 *ECS Meet. Abstr.* MA2015-02 877

[9] Ou J C, Tsai Y Y, Lin T C and et al 2022 *AIP Adv.* 12 065201

[10] Ong J J, Chiu W L, Lee O H and et al 2022 *Materials* 15 1888

[11] Kuo Y H, Tran D P and Ong J J 2022 *J. Mater. Res. Technol.* 18 859-871

[12] Ren H, Yang Y T, Ouyang G and Iyer S S 2021 *ECS J. Solid State Sci. Technol.* 10 0 64008

[13] Ji L, Che F X, Ji H M, Li H Y and Kawano M 2020 *IEEE Trans. Compon. Packag. Manuf. Technol.* 10 2106-2117

[14] Sekhar V N, Kumar M D and Tippabhotla S K 2024 *IEEE ECTC Conf.* 2024-2030

[15] Cheemalamarri H K, Lir J and Lee W 2023 *IEEE EPTC Conf.* 493-497

[16] Ni W, Sheng C, Zhao B, Tian Z, Chen M, Wang S and Wu G 2025 *Mater. Sci. Semicond. Process.* 186 109082

[17] Venable R M, Krämer A and Pastor R W 2019 *Chem. Rev.* 119 5954-5997

[18] Benson N C and Daggett V 2012 *J. Phys. Chem. B* 116 8722-8731

[19] Li D, Zhu Z Y, Zhang Z X and Liu H 2026 *J. Mater. Sci.* 61 8626–8643

[20] Li R, Lei Z Y, Chunmin C M, Zheng H, Wu G and Shen W 2026 *J. Appl. Phys.* 140 035301

[21] Jiménez-Sáez J C, Domínguez-Vázquez J, Pérez-Martín A M C and Jiménez-Rodríguez J J 2002 *Nanotechnology* 13 317-324

[22] Xydou A, Parviainen S and Djurabekova F 2020 *Results Phys.* 16 102890

[23] Wu C D and Liao C F 2025 *J. Phys. Chem. C* 129 16347-16354

[24] Wu C D and Liao C F 2024 *J. Phys. Chem. Solids* 187 111872

[25] Tatsumi H, Kao C R and Nishikawa H 2023 *Sci. Rep.* 13 23030

[26] Hiller D, Tröger D, Grube M, König D and Mikolajick T 2021 *J. Phys. D: Appl. Phys.* 54 275304

[27] Zhang C, Pan Y, Bi Y and Cao X 2023 *Eng. Fract. Mech.* 292 109627

[28] Wang Y, Yang W, Liu X, Lin J and Sun H 2019 *Macromol. Theory Simul.* 28 1900045

[29] Liu H, Ke F J, Pan H and Zhou M 2007 *Acta Phys. Sin.* 56 407-412

[30] Ren Y Q, Wang Y and Lin B 2025 *Jpn. J. Appl. Phys.* 64 065503

[31] Hu Z, Zhang J, Yan Y and et al 2013 *J. Mech. Sci. Technol.* 27 43-46

[32] Uchida K, Tsumura K, Nakamura K, Higashi K, Sugizaki Y and Shibata H 2018 *IEEE I ITC Conf.* 182-184

[33] Shankar U, Gogoi R, Sethi S K and et al 2022 Forcefields Atomist. Simul. (Springer Na ture Singapore, Singapore) pp 299-313

[34] Shankar U, Gogoi R, Sethi S K and et al 2022 Forcefields Atomist. Simul. (Springer Na ture Singapore, Singapore) pp 299-313

[35] Shi Y, Xue Y, Xia D, Wang Y and Wang J 2026 *Appl. Surf. Sci.* 720 165149

[36] Foiles S M, Baskes M I and Daw M S 1988 *Phys. Rev. B* 33 7983

[37] Zhang L, Tian L C, Zhang A L, Jing Y Y and Qu P P 2021 *Int. J. Thermophys.* 42 44

[38] Shan T-R, Devine B D and Kemper T W 2010 *Phys. Rev. B* 81 125328

[39] Yu W, Wu L and Shen S 2017 *Mater. Sci. Eng. A* 695 239-248

[40] Zhang M, Cai H, Zhang J, Li Q, Wang Y, Huang T, Liu J and Wang X 2021 *Corros. Sci.* 182 109275

[41] Shan T-R, Devine B D, Kemper T W, Sinnott S B and Phillpot S R 2010 *Phys. Rev. B* 81 125328

[42] Yu Y 2021 *Mater. Today Commun.* 26 102083